JOURNAL OF Materials CHEMISTRY

Molecularly interconnected SiO_2–GeO_2 thin films: sol–gel synthesis and characterization

Lidia Armelao,*[a] Monica Fabrizio,[b] Silvia Gross,[c] Alessandro Martucci[d] and Eugenio Tondello[c]

[a]*CNR–CSSRCC, via Marzolo 1, Padova, Italy. Phone: +39-49-8275236; Fax: +39-49-8275161; E-mail: armelao@chim02.chin.unipd.it*
[b]*CNR–IPELP, Corso Stati Uniti 4, Padova, Italy*
[c]*Dipartimento di Chimica Inorganica, Metallorganica ed Analitica, Università di Padova, via Loredan 4, Padova, Italy*
[d]*Dipartimento di Ingegneria Meccanica—Sezione Materiali, Università di Padova, via Marzolo 9, Padova, Italy*

Received 7th September 1999, Accepted 17th February 2000
Published on the Web 7th April 2000

SiO_2–GeO_2 films have been synthesized by the sol–gel method starting from an ethanolic solution of $Si(OC_2H_5)_4$ and $Ge(OCH_3)_4$. The coatings have been annealed in air at temperatures ranging between 300 °C and 900 °C. The compositional and microstructural evolution of the samples under thermal annealing has been investigated by X-Ray Photoelectron Spectroscopy (XPS), X-Ray Diffraction (XRD), Secondary-Ion Mass Spectrometry (SIMS) and Atomic Force Microscopy (AFM). Pure and molecularly homogeneous films have been obtained after 300 °C thermal treatment. An amorphous network of interconnected SiO_4 and GeO_4 tetrahedra has been observed up to 700 °C. At higher treatment temperatures the formation of crystalline silica in the cristobalite phase has been detected.

Introduction

In recent years silica glasses containing germanium dioxide have attracted considerable interest due to their various appealing properties. Most of them are strictly related to the composition and to the structure of the glass.[1] Since GeO_2 is well established as the isostructural analogue of SiO_2 and is compatible with the silica network, it is employed as a refractive index modifier in binary xSiO$_2$–(1−x)GeO$_2$ glasses for optics. GeO_2 doped quartz glasses give rise to phenomena such as photosensitive gratings effects and anomalous photo-induced second harmonic generation (SHG).[2,3] Significant attention has been further devoted to the other remarkable optical properties of these binary systems and due to different phenomena. Color centers induced by UV irradiation in Ge-doped SiO_2 glasses are the primary source for the fabrication of several devices with novel photonic functions such as permanent distributed gratings and SHG in optical fibers or planar waveguides.[4] Ge-doped silica glasses have attracted much attention for Bragg gratings, where the photorefractive index change due to the UV induced absorption is employed.[5,6] The photosensitivity exhibited by these materials is ascribable to the presence of germanium dioxide and to the occurrence of germania-related defect centers.[7] Both silica and germania are prototypes of simple glasses consisting of corner-shared TO_4 (T = Si, Ge) tetrahedra linked in a random network structure.[8] T–O–T bond angles are distributed about some most likely value, estimated by X-ray diffraction to be 144° in SiO_2 glass and 133° in GeO_2 glass.[9] Besides structural similarities, a striking difference between these two systems is the concentration of defects. While in pure silica[5] they are of the order of 10^{-9} of the total Si atoms, in pure germania or in binary SiO_2–GeO_2 glasses the concentration is around 10^{-3}–10^{-4} of the total germanium sites. This difference has been ascribed to the different thermodynamic stability between SiO_2 and GeO_2. From a thermodynamic point of view, at room temperature, formation of SiO_2 quartz is favoured with respect to GeO_2 in the hexagonal form. Moreover, the latter is much less stable than SiO_2 and the reduction of GeO_2 to GeO is much easier than that of SiO_2. Under standard conditions, GeO_2 may occur in either the 4-fold coordination of the α-quartz structure, or the 6-fold coordination of the rutile structure. However, although both GeO_2 polymorphs exist at ambient conditions, rutile is the stable structure, whereas the α-quartz structure is metastable.[10] The above considerations apply equally to the two crystalline forms, but not to the glass one, which represents a thermodynamically metastable system.

SiO_2–GeO_2 glasses find further application as material coatings for porous silicon containing ceramics.[11] These coatings improve the oxidation resistance and prevent the so called "pest" oxidation of the material.[12] Finally, for their intrinsic characteristics such as insulating behaviour, low phononic energy with respect to the silicate glasses,[13] transparency and homogeneity, SiO_2–GeO_2 glasses are good candidates as host matrixes for metal or semiconductor clusters for optical applications.

Ge-doped SiO_2 glasses have been prepared by different methods such as Vapor Axial Deposition (VAD),[4,14] ion implantation,[15] CVD[5] and sol–gel.[16] The present paper reports the sol–gel synthesis and characterization of SiO_2–GeO_2 films, at low germania content, starting from solutions of silicon and germanium alkoxides. If GeO_2 is mixed with vitreous silica at a molecular level, Ge atoms would randomly substitute Si atoms in SiO_4 tetrahedra so that the microstructure of the glass would remain a continuous three-dimensional network consisting of interconnected SiO_4 and GeO_4 tetrahedra.[17] Among the synthetic methods, the sol–gel route has gained great interest during recent years for making advanced materials and in particular for preparing oxide-based coatings.[18] The hydrolysis and condensation reactions lead to the formation of oxo-based macromolecular networks giving the unique chance of tailoring the precursor compounds according to the desired process path. This peculiarity, together with the mild conditions of synthesis ("soft chemistry"), makes the sol–gel method particularly suitable for yielding thin films with good control over composition and microstructure. The films and their

This journal is © The Royal Society of Chemistry 2000

thermal evolution have been characterized by SIMS, XPS, XRD and AFM with the aim of contributing to a better understanding of their structure.

Experimental

Precursor solution

A homogeneous, clear, transparent and stable solution was prepared by dissolving germanium tetramethoxide [$Ge(OMe)_4$, TMOG (Aldrich 99.9%)] and tetraethoxysilane [$Si(OEt)_4$, TEOS (Aldrich 99.9%)] in ethanol [C_2H_5OH (Aldrich)]. Molar ratios of TMOG/TEOS/ethanol = 1 : 6.8 : 41.4 were chosen. This solution, stirred for 6 h at room temperature, was hydrolysed by adding doubly distilled water and acetic acid (Aldrich 99.7%) in a molar ratio (TEOS + TMOG)/acetic acid/water = 1 : 0.1 : 3.7. The solution, aged at 60 °C for 10 minutes, appeared clear and stable and was subsequently used for the deposition of the coatings.

Films deposition and characterization

SiO_2–GeO_2 films have been obtained by the dip-coating procedure. Herasil silica slides, 15 × 25 × 1 mm, supplied by Heraeus, were used as substrate. Before use, they were cleaned and rinsed both in doubly distilled water and propan-2-ol. This procedure, repeated several times, is aimed at removing organic residues at the surface and at favouring the best adhesion between coating and substrate.[19] Slides were finally dried in clear air at room temperature. Film deposition was carried out in air with a withdrawal speed of 10 cm min^{-1} and with an external humidity degree of approximately 60%. The films were annealed in air at temperatures ranging between 300 °C and 900 °C for one hour. Transparent, crack-free and colourless samples were obtained after each thermal treatment. The chemical and structural evolution of the films was investigated as a function of the annealing conditions. The composition of the films at the surface and in the bulk was investigated by XPS. XPS spectra were run on a Perkin-Elmer Φ 5600ci spectrometer using non monochromatized Mg-Kα radiation (1253.6 eV). The working pressure was $< 5 \times 10^{-8}$ Pa. The spectrometer was calibrated by assuming the binding energy (BE) of the $Au4f_{7/2}$ line at 83.9 eV with respect to the Fermi level. The standard deviation for the BE values was 0.15 eV. The reported BE were corrected for the charging effects, assigning to the C1s line of adventitious carbon the BE value of 285.0 eV.[20] Survey scans were obtained in the 0–1100 eV range, whereas detailed scans were recorded for the O1s, C1s, Ge3d, Ge2p, Si2p and SiKLL regions. The atomic composition was evaluated using sensivity factors supplied by Perkin-Elmer.[21] Depth profiles were carried out by Ar^+ sputtering at 1.5 keV with an argon partial pressure of 5×10^{-6} Pa. Silicon oxidation state was also evaluated by using the Auger α parameter, defined as the sum of the BE value for the Si2p XPS region and the kinetic energy (KE) of the SiKLL Auger peak.[22]

SIMS analyses, here referred to as SIMS I, were carried out in a custom-built instrument described elsewhere[23] and recently updated. A monochromatic (2 keV, ionic current range between 400 and 800 nA) O_2^+ ion beam collimated to 50 μm was generated in a mass-filtered duoplasmatron ion gun (model DP50B, VG Fisons, UK) and a secondary electron multiplier (90° off-axis) was used for negative- and positive-ion detection in counting mode. Lens potentials, quadrupole electronic control units and detection system were controlled *via* a Hiden HAL IV interface. Surface characterization was carried out recording mass spectra of negative and positive ions respectively on different points of coatings, in order to check composition homogeneity. Subsequently, following the signals of interest as a function of bombarding time, ion species distribution was studied from the surface to the film/substrate interface.

Further SIMS depth profiles for the individual elements, here referred to as SIMS II, were taken using a CAMECA IMS-4F ion microscope equipped with a normal incidence electron gun to compensate for charging effects. Depth profiles were obtained by 14.5 keV Cs^+ bombardment and negative secondary ion detection (beam current = 10 nA, raster area = 125 × 125 μm^2). After reaching the substrate, the thickness of the films was measured by an Alpha-Step 200 Tencor profilometer.

XRD measurements have been performed using a Philips PW 1820 diffractometer (CuKα radiation, 40 kV, 50 mA) equipped with a thin film attachment (glancing angle = 0.5°). Selected angular ranges were step-scanned (0.05°) several times until reaching a satisfactory signal-to-noise ratio.

AFM images were taken using a Park Autoprobe CP instrument operating in contact mode in air. The micrographs were recorded in different areas of each sample, in order to test the film homogeneity. The background was subtracted from the images using the ProScan 1.3 software from Park Scientific.

Results and discussion

A suitable starting system to obtain SiO_2–GeO_2 glasses has proved to be a homogeneous mixture of tetraethoxysilane and germanium tetramethoxide prepared as outlined in the Experimental section. The proper solution composition was optimized by varying both the water and catalyst content in order to achieve a compromise between hydrolysis and condensation rates of the alkoxides. This solution was used for the dip-coating procedure. After deposition, SiO_2–GeO_2 films were thermally treated in air at temperatures ranging between 300 and 900 °C to investigate their compositional and microstructural evolution as well as the behaviour of this system toward crystallization. In this regard, it is well known[24] that crystallization in most glasses proceeds through phase separation followed by nucleation and crystal growth. In these systems, phase separation determines the formation of interfaces and creeks which behave as scattering centers thus compromising the optical properties.

XPS analysis

A detailed analysis of the coatings composition, heat-treated at different temperatures, was firstly carried out by XPS. Concerning film purity, the XPS depth profiles of the C1s peak show that the carbon content of the coatings, mainly deriving from the organic ligands, decreases with increasing treatment temperature. At 300 °C only low atomic percentages (< 3%) of organic residuals are detectable, which are completely removed after some mild sputtering cycles. The observed high purity of the films at relatively low temperatures indicates that, in the adopted experimental conditions, a complete hydrolysis of alkoxides occurs. As regards silicon and germanium, whose atomic ratio is around 5.5 in the various samples, the in-depth distribution of Si2p and Ge3d regions shows the same profile along the film thickness (Fig. 1), so that a common chemical origin of Si and Ge species can be hypothesized. In addition, the BEs of the $Ge2p_{3/2}$, $Ge3d_{5/2}$ and Si2p peaks of the entire series are within the range typical for GeO_2 and SiO_2 and do not show significant differences among the various samples. Experimental BE values for the more intense $Ge3d_{5/2}$ spin–orbit split component of the Ge3d region are centred around 32.7 eV, in agreement with the literature reference value for GeO_2, *i.e.* 32.5 eV.[21] Agreement with germania BE literature values has been found also for the $Ge2p_{3/2}$ peak. The experimental values are centred at 1220.2 eV, typical for GeO_2. Likewise, the BE of the Si2p region (103.6 eV) and the silicon α parameter (1712.0 eV) of the

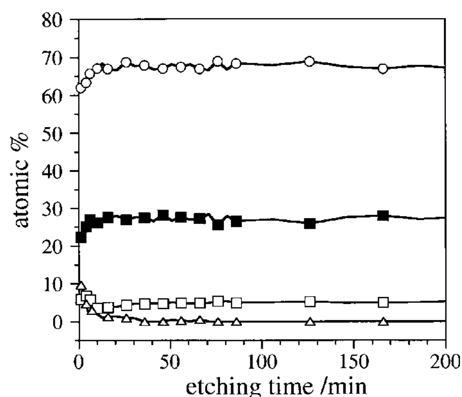

Fig. 1 XPS depth profile for the 300 °C annealed sample. The in-depth distributions of oxygen (○), silicon (■), germanium (□) and carbon (△) are reported.

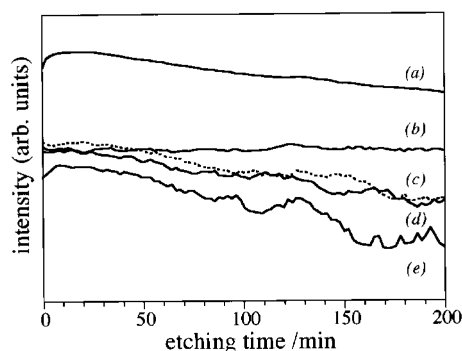

Fig. 2 Positive-ion SIMS depth profile for the 300 °C annealed sample. The in-depth distributions of the various germanium-containing species are normalized to the ^{28}Si signal. The reported fragments are: (*a*) $m/z=74$ ($^{74}Ge^+$), (*b*) $m/z=104$ ($Si_2O_3^+$, $^{72}GeO_2^+$), (*c*) $m/z=118$ ($^{74}GeOSi^+$), (*d*) $m/z=116$ ($^{72}GeOSi^+$) and (*e*) $m/z=134$ ($^{74}GeO_2Si$).

various samples fall within the typical range reported for SiO_2.[20,21] The O1s photoelectronic lines exhibit a symmetric bandshape centred around 532.5 eV without any significant broadening (FWHM ≈ 2.3 eV), and in agreement with the O1s BEs for SiO_2 and GeO_2 (O1s: 532.6 eV in SiO_2, 532.2 eV in GeO_2). These findings have been further confirmed for the 500 °C, the 700 °C and the 900 °C annealed samples. Consequently, considering only the binding energies of XPS silicon- and germanium-related regions an indication of Si–O–Ge moieties is not given.

SIMS analysis

To investigate the formation of Si–O–Ge bonds, typical of the molecularly dispersed glass, SIMS analysis, here referred to as SIMS I, was performed after each thermal annealing. The use of a low-energy sputtering beam, preventing serious structural damage of the investigated surface, allowed a selective fragmentation of the surface species whose detection provides a representative picture of the outer layers. In addition, to obtain the distribution of Ge–Si containing ionic fragments along the film thickness, SIMS depth profiles were recorded. Surface analyses were carried out by detecting and identifying ionic species in the positive ion mass spectra of the annealed samples. Element and species in-depth distribution were studied by following profiles of interesting ion signals as a function of sputtering time. The main ionic species unambiguously identified in the mass spectra of positive ions are: Si_2^+ ($m/z=56$), SiO_2^+ ($m/z=60$), SiO_2H^+ ($m/z=61$), GeO^+ ($m/z=88$), $GeOH^+$ ($m/z=89$), $GeSiO^+$ ($m/z=116$), $GeSiO_2^+$ ($m/z=132$) and $GeSi_2O_2^+$ ($m/z=160$). Signals were attributed by comparing intensity ratios to isotopic patterns by means of isotopic pattern simulation software,[25] which allows the calculation of confidence interval and residual standard deviation for detected species, in order to discriminate different contributions to overlapped signals. Besides the reported silicon- and germanium-containing species, several ionic species characterized by a high ionic yield have been detected on sample surfaces. Most of them derive from decomposition of organic residuals and their contribution progressively decreases as the thermal treatment proceeds. The positive ion mass spectra concerning all the annealed samples show the isotopic patterns related to binary silicon–germanium fragments detected here. It is worth pointing out, besides the $SiOGe^+$ signal, the presence of heavier homologues $GeSi_yO_x^+$, $1 \leqslant x,\ y \leqslant 2$, which suggest the presence of Si–O–Ge direct linkages. In order to analyse the distribution of Ge–Si ionic fragments along the film thickness, the related signals were also followed during bombarding time. The depth profile relative to the $m/z=72$ signal shows an intermediate behaviour between that relative to $m/z=28$, attributed to ^{28}Si, and that associated to $m/z=74$ and assigned to ^{74}Ge, one of the main isotopes of germanium. On account of this, $m/z=72$ can be ascribed to a mixture of Si_2O^+ clusters and $^{72}Ge^+$ ions. It is interesting to compare the germanium-containing species depth profiles normalized to the ^{28}Si signal, in order to discriminate the individual contribution of the single ions. As shown in Fig. 2, particularly meaningful is the similarity among 118/28, 116/28, 134/28 and 74/28 depth profiles, even if the numerical values of the involved intensity ratios are remarkably different. The analogy of these signals evidences their common origin and lead to the assignment of $m/z=116$, $m/z=118$ and $m/z=134$ signals to the germanium-containing species, $^{72}GeOSi$, $^{74}GeOSi$ and $^{74}GeO_2Si$, respectively. On the contrary, the profile of the trace relative to the 104/28 signal appears quite different. This difference can be justified considering that $m/z=104$ can not be entirely attributed to $^{72}GeO_2^+$ clusters, but it includes a particularly marked silicon contribution associated with $Si_2O_3^+$ ionic fragments. The results achieved by the analyses on the 500, 700 and 900 °C annealed samples confirm the picture here described thus validating the formation of direct Si–O–Ge linkages and the molecular dispersion of the elements.

Further SIMS (SIMS II) investigation on the individual elements confirms the homogeneous and uniform distribution of both silica and germania along film thickness. By SIMS II depth profiles, after a sputtering time of 270 s, a remarkable decrease in the intensity of germanium signal of more than one order of magnitude (Fig. 3) indicates the interface film/silica substrate. Consequently, the film thickness was determined by measuring the hole depth through a profilometer, giving a result of 210 ± 2 nm. The standard deviation for this measure, *i.e.* 2 nm, can be assumed as an over-estimate of the average roughness and this value is in close agreement with that measured by AFM, as reported in the following.

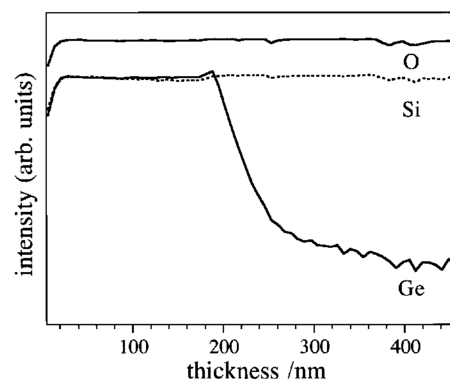

Fig. 3 SIMS depth profile for the 300 °C annealed sample. The in-depth distributions of germanium, silicon and oxygen are reported.

XRD analysis

The microstructural evolution of the films was investigated by XRD which showed an amorphous pattern without any detectable crystalline phase in all the samples up to 700 °C. The 900 °C heat treated sample revealed the presence of crystalline silica. As a matter of fact, the diffraction pattern of the 900 °C annealed sample, reported in Fig. 4, shows peaks located at 21.98° (⟨101⟩) and 36.08° (⟨200⟩) which have been attributed to the SiO_2 cristobalite phase (JCPDS card 39-1425). In particular, the main ⟨101⟩ reflection appears superimposed on the broad band located at about 21.5° which is due to amorphous silica,[26] present both in the films and as a substrate. No peaks ascribed to crystallization of germania were revealed. From the literature concerning the sol–gel preparation of SiO_2–GeO_2 glasses,[27–33] the tendency of GeO_2 gels to crystallize and separate is known. This feature is related to the hydrolysis processes and to the microstuctural homogeneity of the sol. As no GeO_2 phase has been detected, but only SiO_2 cristobalite in the film heated at 900 °C, the formation of a homogeneous phase with a highly interconnected silica–gemania network is supported.

AFM analysis

Concerning the texture and morphology of the film surface, information has been acquired by AFM analysis, a technique commonly used to observe the atomic-scale surface structure of thin layers.[34] AFM micrographs show extremely smooth and uniform surfaces, characterized by an average roughness spanning the interval 1 ± 0.3 nm. In addition, both the surface morphology and average roughness of the samples seem not to be affected by annealing, since no remarkable variation is observed as a consequence of temperature increase. Finally, the acquisition of several images taken on different samples areas proved the homogeneity of the film surfaces.

Conclusions

Pure and molecularly homogeneous SiO_2–GeO_2 thin films have been synthesized *via* sol–gel. The choice of suitable starting solutions of proper precursors has proved to be effective in yielding thin films with good control of the composition. The evolution of the coatings has been studied as a function of thermal annealing performed at different temperatures ($300 \leqslant T \leqslant 900$ °C). XPS investigation showed a high purity of the films at relatively low temperatures (≈ 300 °C). These findings have been justified by assuming that in the adopted experimental conditions complete hydrolysis of the precursors occurs. SIMS analysis evidenced strong correlation and interactions between silicon and germanium in the films. The detection of $GeSi_yO_x^+$ ($1 \leqslant x,\ y \leqslant 2$) fragments strongly supported the existence of direct Si–O–Ge bonds already in the low-temperature treated samples. A partial crystallization occurred only in the 900 °C treated sample, as evidenced by XRD analysis. No peaks associated with crystalline GeO_2 were observed, but only reflections ascribable to the SiO_2 cristobalite phase. These results support the formation of homogeneous films made of molecularly interconnected silica–gemania tetrahedra to form a continuous network.

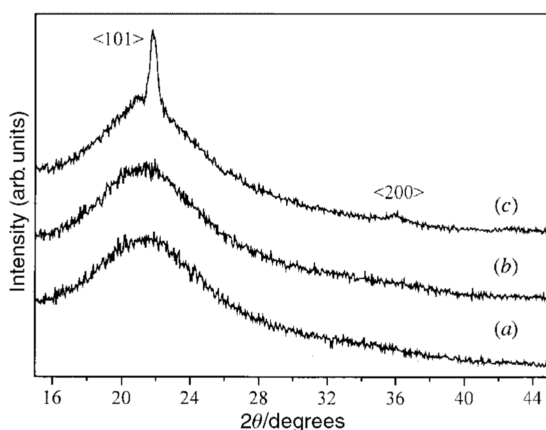

Fig. 4 XRD diffraction patterns for samples heated at (*a*) 300, (*b*) 700 and (*c*) 900 °C. The observed reflections belong to the SiO_2 cristobalite phase, as reported in the JCPDS card 39-1425.

Acknowledgements

This work was partially funded by Progetto Finalizzato "Materiali Speciali per Tecnologie Avanzate II" of the CNR (Rome). Thanks are due to Professor F. Caccavale for SIMS II analysis and helpful discussion.

References

1 S. K. Sharma, D. W. Matson, J. A. Philpotts and T. L. Rousch, *J. Non-Cryst. Solids*, 1984, **68**, 115.
2 K. O. Hill, Y. Fujii, D. C. Johnson and B. S. Kawasaki, *Appl. Phys. Lett.*, 1978, **32**, 647.
3 U. Österberg and W. Margulis, *Opt. Lett.*, 1986, **11**, 516.
4 J. Nishii, A. Chayahara, K. Fukumi, K. Fujii, H. Yamanaka, H. Hosono and H. Kawazoe, *Nucl. Instrum. Methods*, 1996, **B116**, 150.
5 H. Hosono, Y. Abe, D. L. Kinser, R. A. Weeks, K. Muta and H. Kawazoe, *Phys. Rev.*, 1992, **B46**, 11445.
6 J. Nishii, K. Fukumi, H. Yamanaka, K. Kawamura, H. Hosono and H. Kawazoe, *Phys. Rev.*, 1995, **B52**, 1661.
7 J. Stone, *J. Appl. Phys.*, 1987, **62**, 4371.
8 J. Neuefeind and K. D. Liss, *Ber. Bunsenges. Phys. Chem.*, 1996, **100**, 1341.
9 J. A. Wong and C. A. Angell, *Glass Structure by Spectroscopy*, Marcel Dekker, New York, 1976, p. 409.
10 K. M. Ault and R. A. Secco, *Solid State Commun.*, 1996, **98**, 449.
11 J. Schlichting and S. Neumann, *J. Non-Cryst. Solids*, 1982, **48**, 185.
12 J. Schlichting, *Blech Rohre Profile*, 1979, **26**, 226.
13 R. Reisfeld and C. K. Jørgensen, *Excited state phenomena in vitreous material*, Elsevier, Amsterdam, 1987, pp. 1–90.
14 M. Fujimaki, T. Watanabe, T. Katoh, T. Kasahara, N. Miyazaki, Y. Ohki and H. Nishikawa, *Phys. Rev.*, 1998, **B57**, 3920.
15 J. Albert, K. O. Hill, D. C. Johnson, J. L. Brebner, Y. B. Trudeau and G. Kayris, *Appl. Phys. Lett.*, 1992, **60**, 148.
16 K. D. Simmons, G. I. Stegeman, B. G. Potter Jr. and J. H. Simmons, *J. Non-Cryst. Solids*, 1994, **179**, 254.
17 M. Okundo, C. D. Yiu, H. Morikawa, F. Marumo and H. Oyanagi, *J. Non-Cryst. Solids*, 1986, **87**, 312.
18 C. J. Brinker and G. W. Scherer, *Sol–Gel Science: The Physics and Chemistry of Sol–Gel Processing*, Academic Press, New York, 1990.
19 L. Armelao, R. Bertoncello, S. Coronaro and A. Glisenti, *Science and Technology for Cultural Heritage*, 1998, **7**, 41.
20 D. Briggs and M. P. Seah, *Practical Surface Analysis*, 2nd Edition, Wiley, New York, 1990, vol. 1, p. 543.
21 J. F. Moulder, W. F. Stickle, P. E. Sobol and K. D. Bomben, in *Handbook of X-Ray Photoelectron Spectroscopy*, ed. J. Chastain, Perkin-Elmer Corporation, Eden Prairie, MN, 1992.
22 C. D. Wagner, *Anal. Chem.*, 1972, **44**, 972.
23 C. Pagura, S. Daolio and B. Facchin, in *Secondary-Ion Mass Spectrometry SIMS VIII*, ed. A. Benninghoven, K. T. F. Jansen, J. Tumpner and H. W. Werner, Wiley, Chichester, 1992, p. 239.
24 P. W. McMillan, *Glass Ceramics*, Academic Press, New York, 1979.
25 C. Pagura and S. Valcher, personal communication.
26 R. K. Iler, *The Chemistry of Silica*, Wiley, New York, 1979.
27 D. G. Chen, B. G. Potter and J. H. Simmons, *J. Non-Cryst. Solids*, 1994, **178**, 135.
28 M. Yamazaki and K. Kojima, *J. Mater. Sci. Lett.*, 1995, **14**, 813.
29 S. Shibata, T. Kitagawa, F. Hanawa and M. Horiguchi, *J. Non-Cryst. Solids*, 1986, **88**, 345.
30 S. P. Mukherjee, *J. Non-Cryst. Solids*, 1986, **82**, 293.
31 Y. Kanno and J. Nishin, *J. Mater. Sci. Lett.*, 1993, **12**, 10.
32 S. P. Mukherjee, *Mater. Res. Soc. Symp. Proc.*, 1986, **73**, 443.
33 G. Brusatin, M. Guglielmi and A. Martucci, *J. Am. Ceram. Soc.*, 1997, **80**, 3139.
34 K. L. Westra and D. J. Thomson, *Thin Solid Films*, 1995, **257**, 15.